ACS Sustainable Chemistry & Engineering

Research Article

pubs.acs.org/journal/ascecg

Effluent Gas Flux Characterization during Pyrolysis of Chicken Manure

Sydney C. Clark,[†,‡] Rebecca Ryals,[*,‡,§] David J. Miller,[‡] Charles A. Mullen,[∥] Da Pan,[⊥] Mark A. Zondlo,[⊥] Akwasi A. Boateng,[∥] and Meredith G. Hastings[†,‡]

[†]Department of Earth, Environmental and Planetary Sciences, Brown University, 324 Brook Street, Providence, Rhode Island 02912, United States

[‡]Institute at Brown for Environment and Society, Brown University, 85 Waterman Street, Providence, Rhode Island 02912, United States

[§]Department of Natural Resources and Environmental Management, University of Hawaii, 1910 East-West Road, Honolulu, Hawaii 96822, United States

[∥]Eastern Regional Research Center, Agricultural Research Service, U.S. Department of Agriculture, 600 East Mermaid Lane, Wyndmoor, Pennsylvania 19038, United States

[⊥]Department of Civil and Environmental Engineering, Princeton University, 59 Olden St, Princeton, New Jersey 08540, United States

Supporting Information

ABSTRACT: Pyrolysis is a viable option for the production of renewable energy and agricultural resources from diverted organic waste streams. This high temperature thermochemical process yields material with beneficial reuses, including bio-oil and biochar. Gaseous forms of carbon (C) and nitrogen (N) are also emitted during pyrolysis. The effluent mass emission rates from pyrolysis are not well characterized, thus limiting proper evaluation of the environmental benefits or costs of pyrolysis products. We present the first comprehensive suite of C and N mass emission rate measurements of a biomass pyrolysis process that uses chicken manure as the feedstock to produce biochar and bio-oil. Two chicken manure fast pyrolysis experiments were conducted at controlled temperature ranges of 450−485 °C and 550−585 °C. Mass emission rates of nitrous oxide (N_2O), nitric oxide (NO), carbon monoxide (CO), carbon dioxide (CO_2), methane (CH_4), and ammonia (NH_3) were measured using trace gas analyzers. Based on the system mass balance, 23−25% of the total mass of the manure feedstock was emitted as gas, while 52−55% and 23% were converted to bio-oil and biochar, respectively. CO_2 and NH_3 were the dominant gaseous species by mass, accounting for 58−65% of total C mass emitted and 99% of total reactive N mass emitted, respectively. Temperature variations within the two set of temperature ranges had a perfunctory effect on bio-oil production and gaseous emissions, but the higher temperature range process produced more bio-oil and slightly less emissions. However, a larger effect on the relative amounts of CO and CO_2 produced were observed between the different temperature regimes. These results have important implications for greenhouse gas and reactive N life cycle assessments of biochar and bio-oil.

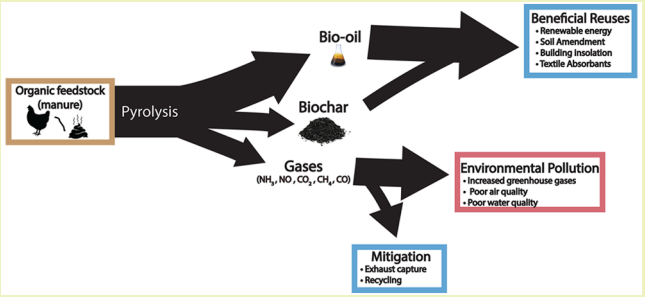

KEYWORDS: *biochar, pyrolysis, gas flux, poultry char, greenhouse gases, chicken manure*

INTRODUCTION

Biochar is a byproduct of pyrolysis (anaerobic) or gasification (aerobic) thermal decomposition processes of organic matter. While pyrolysis and gasification technologies have been in use for decades, these processes have received greater attention in recent decades as bio-oil and/or syngas could be used as a renewable biofuel alternative to fossil fuels and biochar soil amendments could reduce the negative consequences of fertilizer for air quality, climate change, and aquatic and terrestrial acidification.[1,2] Biochar has revealed promise in promoting carbon (C) sequestration,[3−5] minimizing greenhouse gas emissions,[6,7] increasing soil fertility,[8] and crop productivity,[6,8] increasing water availability in drought-prone conditions,[9] increasing bioavailability of adsorbed ammonia[10] and preventing nutrient leaching.[11] In addition, biochar products minimize volume and mass of the original feedstock,[12] reducing transportation costs of organic waste resources.

Biochar has been produced from many organic feedstocks, including grasses, woody biomass, and manures.[3,12,13] Manure-based biochar use could mitigate greenhouse gas emissions and reactive nitrogen (Nr) pollution to air and water from concentrated animal feeding operations.[14] Fast pyrolysis of

Received: March 16, 2017
Revised: June 4, 2017
Published: July 17, 2017

DOI: 10.1021/acssuschemeng.7b00815
ACS Sustainable Chem. Eng. XXXX, XXX, XXX−XXX

organic feedstocks for biochar produces bioenergy resources (i.e., bio-oil) that can displace a portion of fossil fuel-based energy, and biochar as a coproduct.[15]

While evidence for pyrolysis product benefits for agriculture and renewable energy is mounting, a key uncertainty remains in the assessment of their biogeochemical life cycle impacts. The magnitude and forms of mass emission rates during pyrolysis of organic feedstocks to produce biorenewable products are not well quantified. Carbon gases emitted during pyrolysis include major greenhouse gases: carbon dioxide (CO_2), methane (CH_4), and air pollutant carbon monoxide (CO). Nitrogen gases emitted during pyrolysis include nonreactive dinitrogen (N_2), as well as several forms of Nr such as ammonia (NH_3), nitrous oxide (N_2O), and nitrogen oxides (NO_x). Reactive forms of N have cascading impacts on environmental systems and human health.[2,16] Therefore, it is critical to understand the potential unintended losses of C and N during the production of biochar and bio-oil in order to assess the net benefits of its utility for mitigating climate change and/or Nr pollution, particularly from high N-content feeds such as chicken manure.[17] In this study, we measure total C and Nr mass emission rates during fast pyrolysis of chicken manure to quantify and characterize the dominant Nr and C species emitted during the pyrolysis process. Experiments were conducted at two temperature ranges (450−485 °C and 550−585 °C) to determine the effect of temperature as a proximal control on mass emission rates. This work constitutes some of the first C and Nr mass emission rates during the pyrolysis of chicken manure to produce bio-oil and biochar, which can be compared with future experiments under different conditions. These measurements provide a foundation for future C and N life cycle analyses, which can address applicability of this technology at large and small scales and analyze the cost benefit of reducing manure in pollution hotspots.

EXPERIMENTAL (MATERIALS AND METHODS)

Experimental Design. Effluent gas fluxes of Nr species (NO and NH_3), greenhouse gases (N_2O, CH_4, and CO_2), and carbon monoxide (CO) were measured during the pyrolysis of chicken manure. Chicken manure was collected from conventional broiler poultry production houses raising the Cobb chicken breed with unlimited grain feed rations according to standard industry practices (Frye Poultry, West Virginia). Manure consisted of fresh scrapings of house floors and included chicken manure and sawdust.[18] All manure was dried, sieved and homogenized to 2 mm grain size for pyrolysis efficiency[13] (see sections: Exp 1: Low Temperature (450−485 °C and Exp 2: High Temperature (545−585 °C) for more details). Small particles are needed for rapid heat transfer to the entire biomass material for fast pyrolysis.[19]

Manure was pyrolyzed using U.S. Department of Agriculture's bubbling fluidized bed pyrolysis development unit (PDU) located at the Eastern Regional Research Center (Wyndmoor, PA). The reactor bed consisted of a 7.6 cm diameter pipe filled to static bed depth of 20 cm sand, heated electrically to the temperatures mentioned above. Manure was fed by an auger directly into a bubbling sand bed fluidized with N_2. The entrained pyrolysis solids and vapors travel to a cyclone separator where the biochar is removed from the vapor stream and collected. The vapors continue onto a train of four chilled condensers in series to remove condensable vapors followed by two electrostatic precipitators used for capturing aerosols. This pyrolyzer is capable of producing bio-oil under variable temperature conditions, with the additional coproducts of this process including biochar and non-condensable gas (NCG). A detailed description of the bench-scale pyrolysis instrument used, evidence of fast pyrolysis efficiency using 2 mm grain size and controls on exhaust flow rate is available in Boateng et al. 2007.[13]

Two experiments were conducted starting with a fully cleaned pyrolyzer. Experimental conditions for each run are provided in Table 1. Temperature was set at 450−485 °C (low temp, exp 1) and at 550−585 °C (high temp, exp 2) and constraints were placed on feed rate, N_2 dilution and flow rate. A TGA study shows that chicken manure experiences maximum loss at similar temperatures to most lignocellulosic biomass.[20] It has also been well established that temperatures between 450 and 600 °C maximize bio-oil production for biomass,[19] and the temperatures chosen provide two regimes within this range to evaluate emissions associated with fast pyrolysis of chicken manure. However, future work should consider testing the effect of other temperature ranges, as well as repeatability on gas effluent during this process.

Table 1. Experimental Conditions, Product Masses and Percent Composition by Mass from Pyrolysis of Chicken Manure

experimental constraints	Exp 1	Exp 2
temp range (°C)	450−485	546−588
run time (minutes)	110	159
average feed rate (kg/h)	2.78	2.11
average N_2 Dilution (L/min)	80	93
manure moisture (%)	27.21	27.51
product masses post pyrolysis	**Exp 1**	**Exp 2**
biochar (kg)	0.825	1.14
bio-oil (kg)	0.378	0.838
gas (kg)	0.711	1.10
biochar (% composition by mass)	23.3	23.2
bio-oil (% composition by mass)	51.9	54.6
gas (% composition by mass)	25.0	23.3

Gas Measurements. Trace gas concentration measurements were performed using an open-path quantum cascade laser for NH_3,[21] cavity ring-down spectroscopy for CH_4 and CO_2 (Picarro, model G2301), ICOS (integrated cavity output spectroscopy) for CO and N_2O (Los Gatos Research, model 907−0014); and chemiluminescence for NO and NO_x (ThermoFisher Scientific, Model 42i analyzer). The NH_3 sensor provides 0.1 s resolution concentration measurements and retrievals were calibrated before and after experiments from 10 ppbv (ambient NH_3) to 9 ppmv NH_3 to within 0.20 ppbv ±20% using methods described in Miller et al. (2014).[21] Linear calibration curve fitting was applied up to 2 ppmv and logarithmic fitting from 2 to 9 ppmv NH_3. Above 9 ppmv NH_3, concentrations were estimated using offline spectral fitting of direct absorption spectra up to a maximum of 12 ppmv NH_3 (assuming nonlinear absorption with concentration in this range as optical saturation limits were approached).[21] CH_4, N_2O and CO were measured at 1 s and CO_2 at 5 s resolution. The precision of these measurements is discussed in section Mass Balance and Gas Flux Uncertainties. The NO_x Analyzer was used for 8 s resolution NO and NO_x measurements and were calibrated to within ±5% accuracy using a dilution calibrator (ThermoFisher Scientific, model 146i): using 50.2 ppmv NO in N_2 and 10 ppmv NO_2 in N_2 gas standards diluted with zero air (ThermoFisher Scientific, model 111) over a range from 0 to 500 ppbv NO_x. All data was recorded in real-time by a laptop computer.

All gases were captured within a static flux chamber designed to enclose the NH_3 sensor and a three-stage measurement process (2−3 min per stage) was conducted as follows: (1) NH_3 desorption flux from the chamber surface was monitored before introducing the flux to the chamber, (2) fluxes for all gaseous species were measured, and (3) NH_3 adsorption onto the chamber walls was monitored while flux to the chamber stopped. A slipstream of gas exhaust (typical slipstream flow rate was ~150 mL min^{-1}) was piped from the pyrolyzer to a 6.5 L static flux chamber using one PTFE Teflon tubing (1/8″ ID x 1/4″ OD) where all gases could be measured simultaneously at the same

DOI: 10.1021/acssuschemeng.7b00815
ACS Sustainable Chem. Eng. XXXX, XXX, XXX−XXX

inlet. Two PTFE particle filters (1.0 μm, 47 mm) were used to remove particulate matter from the exhaust slipstream prior to entering the chamber. The total exhaust flow rates were 80 or 93 L min^{-1} during experiments one and two, respectively. The flow rate was increased for the second experiment in an effort to dilute the analyte gases (particularly NH_3) to provide a better concentration range for the NH_3 sensor. Both flow rates provided residence times appropriate for fast pyrolysis and were not expected to have a significant effect on the chemical reactions (although examining the impact of flow rate variability on gas fluxes could be considered in future research). During the flux measurements, a microcontroller unit (Arduino Uno) recorded temperature, pressure and relative humidity simultaneously within the flux chamber with a digital relative humidity and temperature sensor (HYT 271, IST Innovative Sensor Technology, accuracy ±1.8% RH and ±0.2 C) as well as a digital pressure sensor (MS5803−01BA, Measurement Specialties Inc., accuracy ±0.5 hPa). Exhaust temperature ranged from 23.7−29.3 °C, pressure was steady at 999.48 ± 1 hPa and relative humidity ranged from 25−59%.

Exp 1: Low Temperature (450−485 °C). The first batch of manure was sieved and homogenized to 2 mm grain size using a seven-bladed Wiley Mill (Thomas Scientific, model 4, Swedesboro, NJ). All manure was sealed and stored at room temperature until pyrolysis measurements could take place (<1 month since collection). Storage times were kept to a minimum to reduce potential ammonia volatilization and changes in N content. Manure was kept tightly sealed and stored in buckets lined with compostable bags. There were no obvious signs of decomposition during storage. After the fluidized bed was heated to 450−485 °C, manure was incorporated into the feedstock funnel at a constant rate and the primary gas stream was diluted with N_2 (Table 1). Over 110 min, 10 flux measurements (6−8 min per chamber measurement) were taken of all six gaseous species. The first three measurements reflect background levels prior to any chicken manure feedstock addition, which occurred at around 40 min.

Exp 2: High Temperature (545−585 °C). The second batch of manure was oven-dried at 60 °C overnight and then homogenized using the Wiley Mill to 2 mm grain size to produce a drier feedstock. A drier manure is less likely to slow pyrolysis reactions and will make the process more efficient. Fluidized bed temperatures were set from 550−585 °C using drier manure to conduct mass emission rate measurements under a steady feed rate and N_2 dilution (Table 1). Over 159 min, 18 flux measurements were (6−8 min per chamber measurement) were taken of all six gaseous species with the first four measurements reflecting background levels before the addition of feedstock at around 40 min.

Subsamples of manure, biochar and bio-oil were weighed, oven-dried at 60 °C overnight and reweighed to calculate the moisture content for each experiment. These samples were analyzed for percent total organic C and total N using Elemental Analysis (Thermo EA1112 CHNS/O Analyzer), which were used for mass balance calculations. The uncertainties of C and N content estimates from elemental analysis were quantified by the standard deviation (1σ) between multiple replicate samples for each pyrolysis coproduct as well as the original biomass for each experimental batch with mean %C or %N ± 1σ reported in Supporting Information (SI) Table S1.

Mass Balance Approach. Exhaust losses were also calculated using a mass balance approach. With known initial masses of manure and final masses of biochar and bio-oil, initial and final masses of C and N were calculated using the following equations:

$$I_{\mathrm{Cmass}} = I_{\mathrm{dry\,manure}} \times \left(\frac{P_{\%\mathrm{Cmanure}}}{100}\right) \tag{1}$$

$$F_{\mathrm{Cmass}} = F_{\mathrm{biochar\,mass}} \times \left(\frac{P_{\%\mathrm{Cbiochar}}}{100}\right) \tag{2}$$

where $I_{\mathrm{C\ mass}}$ is the initial manure C mass, $I_{\mathrm{dry\ manure}}$ is the initial mass of manure prior to pyrolysis, $P_{\%\mathrm{C\ manure}}$ is the %C of manure, $F_{\mathrm{C\ mass}}$ is the final biochar C mass, $F_{\mathrm{biochar\ mass}}$ is the final mass of biochar post pyrolysis and $P_{\%\mathrm{C\ biochar}}$ is %C of the biochar. These were used to calculate losses (from the system) in total C mass (3) and total N mass (4). Total mass lost is the gas estimated from the difference in N_2 input−N_2 output from the GC used at the USDA facility, whereas C and N mass loss are calculated by difference from that contained in the bio-oil and biochar.

$$\text{total C mass lost} = \text{initial manure C} - \text{final biochar C} - \text{final bio-oil C} \tag{3}$$

$$\text{total N mass lost} = \text{initial manure N} - \text{final biochar N} - \text{final bio-oil mass N} \tag{4}$$

Uncertainty in mass loss differences was calculated using error propagation for mass balance using eq 5, where δa, δb, and δc is the uncertainty associated with C or N for manure, biochar and bio-oil, respectively and results are shown in SI Table S2.

$$\delta\mathrm{Nor}\delta C = \sqrt{\delta a^2 + \delta b^2 + \delta c^2} \tag{5}$$

Effluent Gas Flux Approach. Gas flux measurements were used to calculate total mass emitted for each C and N species. First, all gas analyzer timestamps were synchronized to the laptop computer time before recording data. Each flux measurement period was picked out of the time series during rising gas concentrations. A single gas (NO) was selected to ensure appropriate temporal alignment of the fluxes for synchronous flux calculations. Least squares linear regression was used to estimate the slope of each concentration time series and assumed that the slope was constant during the 2−3 min of each chamber measurement. The mass emission rate of each C and N species in kilograms N or C per minute (kg min^{-1}) was determined using

$$E = \frac{VP}{RT} \times \frac{\mathrm{d}c}{\mathrm{d}t} \times \mathrm{mw} \tag{6}$$

where V was the fixed volume of the flux chamber (6.5 L or 0.0065 m^3), P and T were measured pressure (1 atm) and temperature (25 °C), $\frac{\mathrm{d}c}{\mathrm{d}t}$ was defined as the slope of the regression fit (ppmv min^{-1}) and mw is the molecular weight of the corresponding element (C or N) in g mol^{-1}.

The adsorption and desorption flux monitoring was conducted to evaluate how the surface affinity of NH_3 affected the chamber measurements. For a majority of flux measurements, within 1 min of beginning the flux stage NH_3 inside the chamber reached levels of optical absorption saturation above which concentrations could not be retrieved and flux corrections could not be performed. However, based on measurements below these limits, NH_3 concentrations (>10 ppmv) during flux measurements were higher than the wall saturation point and adsorption was the dominant process for NH_3 losses. For all gases, we scaled the flux chamber measurements to the total exhaust stream using the ratio of total exhaust to slipstream flow. During experiment one, the slipstream flow rate was stable at 150 mL min^{-1}. However, flow was more difficult to stabilize during the second experiment due to issues with filter clogging in the line, but was typically 309 mL min^{-1}. Periodic flow measurements with a flow meter (Dry Cal Pro, MesaLabs, model Defender 520) were linearly interpolated to estimate flows across the emission measurement period (SI Table S3). The total emission mass uncertainties were quantified. Each flux measurement uncertainty was estimated using the root mean squared error (RMSE) of the regression slope as in Laville et al. (2011)[22] (SI Table S4). The mass emission rate time series was integrated across the experimental period to obtain total mass (kg N or C) of each species emitted. The total mass of N and C gases were compared with the mass balance results to assess differences between both methods of calculating gaseous loss. Uncertainty in mass loss differences were calculated using the average gas emission rate and the experimental time duration to characterize total mass emitted (SI Table S5), at which point mass uncertainty was calculated by taking into account the instrumental error (δF) to calculate the δM for each gas measured (SI Table S5). Total N and C error was propagated using eq 5, where δa, δb and δc were uncertainties associated with each species (Table S5). After propagating the elemental error separately by approach (MB vs GF), the total error for C and N between methods was calculated using the same approach (Table S6). Differences might reveal whether

DOI: 10.1021/acssuschemeng.7b00815
ACS Sustainable Chem. Eng. XXXX, XXX, XXX−XXX

the gases we measured account for most of the gaseous losses or if our measurements are missing gases such as organic N, other NO_y, particulate ammonium nitrate, hydrocarbons or organic particulates not removed by precipitators. All data processing was performed using a commercial software package (MATLAB 8.6, The MathWorks Inc., Natick, MA, R2015b).[23]

RESULTS

Pyrolysis product masses and experimental conditions shown in Table 1 show that differences between experimental conditions resulted in similar outcomes for the redistribution of mass by product. As shown in Table 1, the percent composition by dry mass of each product was 23% (biochar), 25% (gas), and 52% (bio-oil) for experiment 1 and 23% (biochar), 23% (gas), and 55% (bio-oil) for experiment 2. The manure moisture contents were ~27% in both experimental batches (Table 1), which suggests that the predrying treatment for the second batch was either ineffective at creating a drier manure or the initial manure moisture was greater than 27%. While C and N gases were the focus of this study, ash content and other elements (hydrogen, oxygen and sulfur) were characterized on a dry-basis mass (see SI Table S1).

C & N Emissions by Mass Balance. C and N dry-basis, percent composition of each coproduct had lower %C and %N contents for manure, biochar and bio-oil in experiment 1 compared to experiment 2 (SI Table S1). Standard deviations for %C and %N were 0.84% or less for all measurements (SI Table S1). Mass balance calculations suggest that 0.71 kg (27.6%) of the total initial manure mass was emitted as mostly gas during the pyrolysis process, but small amounts of particulate matter, uncondensed reaction water and uncondensed volatile organics are also emitted. There was a 0.562 kg mass loss as some form of C (51.1% of input C), while there was only a 0.052 kg mass loss as some form of Nr (52% of input N) (Table 2). Mass balance calculations indicate that

Table 2. Mass balance calculations illustrating mass losses using biochar, manure and bio-oil components for experiments 1 and 2

	Exp 1		Exp 2	
mass loss calculations from mass balance	kg	%	kg	%
initial manure mass, dry (kg)	2.574		4.075	
initial manure C mass (kg)	1.098		1.720	
initial manure N mas (kg)	0.099		0.165	
final biochar mass, dry (kg)	0.825		1.140	
final biochar C mass (kg)	0.274	24.9%	0.486	28.2%
final biochar N mass (kg)	0.017	17.1%	0.035	21.1%
final bio-oil mass, dry (kg)	0.378		0.838	
final bio-oil C mass (kg)	0.263	23.9%	0.611	35.5%
final bio-oil N mass (kg)	0.028	28.8%	0.071	23.0%
total mass lost (kg)	0.711		1.104	
total C mass lost (kg)	0.562	51.1%	0.623	36.2%
total N mass lost (kg)	0.052	52.5%	0.059	35.7%
total C + N mass lost (kg)	0.614	51.3%	0.682	36.1%

1.104 kg (23.3%) of total mass was lost during pyrolysis in experiment 2 (Table 2). Of this total mass, there was a 0.623 kg (36.6%) emission of C and a 0.059 kg (36.2%) emission of N (Table 2).

C & N Emissions by Effluent Gas Flux. During experiment 1, produced CO_2 and NH_3 were the highest source of gas emissions (Table 3 and SI Table S7) for C and N species

Table 3. Total Masses of Each Element by Species Emitted (e.g C Content of CO_2 Emitted) For Experiment 1 Over 110 min Scaled by the Ratio of Slipstream:Full Exhaust Flow[a]

gas	total mass (kg C or N)	% C or N mass of measured gases
CO_2–C	5.2×10^{-02}	66
CH_4–C	4.2×10^{-03}	5.2
CO–C	2.3×10^{-02}	29
total C	8.0×10^{-02}	100.2
NO–N	3.3×10^{-05}	0.34
N_2O–N	7.4×10^{-06}	0.08
NH_3–N	9.7×10^{-03}	99
total N	9.7×10^{-03}	99.42
ratio of slipstream: full flow	85L min^{-1}:150 mL min^{-1}	566.667
C+N mass lost	8.9×10^{-02}	
total C mass lost (kg)	8.0×10^{-02}	
total N mass lost (kg)	9.7×10^{-03}	
missing C (kg)	4.8×10^{-01}	
missing N (kg)	4.2×10^{-02}	

[a]Gas emissions were broken down by the percent measured of the total composition using total mass emitted as kg C or kg N. See SI Table S4 for experiment 2 results. C+N mass lost is the cumulative gas emissions.

measured, respectively, which equates to 66% of total C emissions as CO_2 and ~99% of total N as NH_3 gaseous emissions measured (Table 3). The next prominent emissions were as CO and CH_4 for carbon and NO and N_2O for nitrogen (Table 3 and SI Table S7). The total C and N mass emitted during pyrolysis (of what we measured in the gas phase) was 0.089 kg (Table 3). Of this mass, 0.080 kg was emitted as total C and 0.010 kg was emitted as total N (Table 3). Carbon species (CO_2, CH_4 and CO) accounted for 66%, 5.2% and 29% of the total C emissions (Figure 1; Table 3). Nitrogen species (NO, N_2O and NH_3) comprised 0.34%, 0.08% and 99% of total N emissions (Figure 1; Table 3). These compositions are further illustrated by mole percent for entire gas emissions for both C and N (SI Figure S1, panels a, c).

Similar patterns were observed in gaseous abundance and composition of the pyrolysis exhaust during both experiments

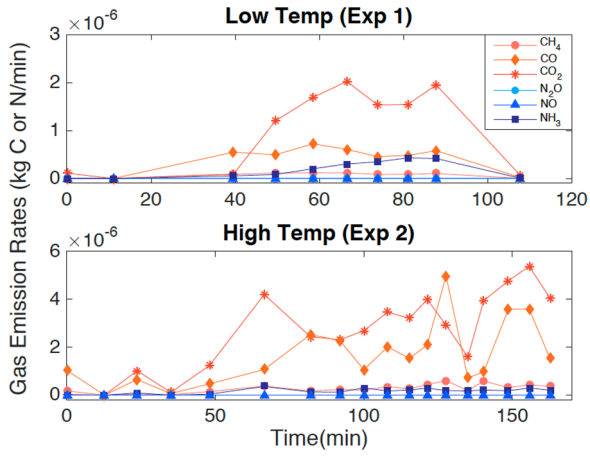

Figure 1. Gas flux time series during Low Temp (exp 1) and High Temp (exp 2) of each gas species in kg C or N/min. N_2O is not present in the second experiment because measurements indicated that fluxes were near zero. Note the change in scales for experiment 2. Feedstock was introduced at 40 min after initial background gas levels were recorded.

DOI: 10.1021/acssuschemeng.7b00815
ACS Sustainable Chem. Eng. XXXX, XXX, XXX−XXX

where CO_2 and NH_3 had the highest emissions (SI Tables S7 and 4). Using the area of the total mass emitted, the total C and

Table 4. Masses of Each Element by Species Emissions (e.g C Content for CO_2) for Experiment 2[a]

gas	total mass (kg C or N)	% C or N mass of measured gases	
CO_2–C	1.2×10^{-01}	58	
CH_4–C	1.2×10^{-02}	5.9	
CO–C	7.3×10^{-02}	36	
total C	2.0×10^{-01}	99.68	
NO-N	5.3×10^{-05}	0.68	
NH_3–N	7.8×10^{-03}	99	
total N	7.8×10^{-03}	99.42	
ratio of slipstream: average full flow	93L min^{-1}: 309 mL min^{-1}		301.113
C+N mass lost	2.1×10^{-01}		
total C mass lost (kg)	2.0×10^{-01}		
total N mass lost (kg)	7.8×10^{-03}		
missing C (kg)	4.2×10^{-01}		
missing N (kg)	5.2×10^{-02}		

[a]The calculated ratio of slipstream:full exhaust flow was used in tandem with the integrated area of each gaseous element to calculate the total mass emitted during the experimental period by gas and element. Slipstream flow rate was ~309 mL min^{-1} Gas emissions were broken down by the percent measured of the total composition using total mass emitted as kg C or kg N. C+N mass lost is the cumulative gas emissions.

N mass emissions were 0.21 kg during experiment 2 (Table 4). Of this mass, 0.20 kg was lost as total C and 0.0078 kg was lost as total N (Table 4). The relative variations of all gas emission rates were very similar between experiments and total mass emitted was higher for the longer second experiment (Figure 1; SI Table S7 and Table 4). CO_2, CH_4, and CO accounted for 58%, 5.9%, and 36% of the C emissions measured (SI Figure S2; Table 4). N_2O, NO, and NH_3 comprised 0%, 0.68%, and 99% of total N emissions measured (SI Figure S2; Table 4). Elemental composition is represented for both C and N in mole percent, which further demonstrates that CO_2, CO and NH_3 are the dominant gaseous components for C and N (SI Figure S1, panels b, d). The concentrations of N_2O were near ambient atmospheric concentrations in the flux chamber during experiment 2, therefore are not currently incorporated into the emission calculations for the second experiment. The percent differences in emission rates between the first (lower temperature) and second (higher temperature) experiments were −7.3% for CO_2, + 0.65% CH_4, and +6.7% for CO while NO changed by +0.33% and −0.32% for NH_3.

Mass Balance vs Effluent Gas Flux. The gas flux approach produced estimates of total mass losses, which were a factor of 3−6 (for carbon) and 5−8 (for nitrogen) lower than those calculated from the mass balance approach. Mass loss differences/deficits for C+N mass, total C mass and total N mass between the two methods are as follows: 0.525 (43.8% of total input), 0.482 (43.9%) and 0.042 kg (42.4%) for low temperature conditions (Figure 2, SI Table S8) while mass loss differences appear much lower during high temperature conditions of experiment 2 (0.470 kg or 24.9%, 0.419 or 24.3%, and 0.051 kg or 30.9%) for C+N mass, total C and total N − Figure 2, SI Table S8). The discrepancies between each method potentially suggest that the gas flux method underestimates mass loss compared to the mass balance approach and/or that the mass balance approach is overestimating the

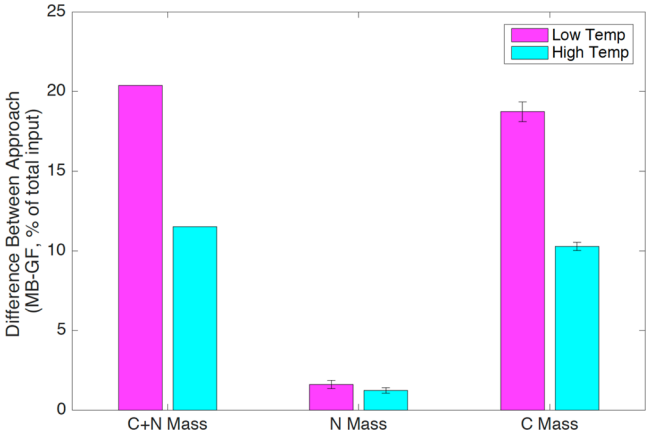

Figure 2. C+N mass, total mass as C and total mass as N differences (% of total dry input; exp 1:2.574 kg, exp 2:4.075 kg) between mass balance and gas flux approaches used for each experiment (1 = magenta, 2 = cyan) discussed in section Mass Balance vs Gas Flux. Errors were derived from propagation of both mass balance and gas flux approach uncertainties (explained in section Mass Balance and Gas Flux Uncertainties).

emissions. It is likely that the gas flux measurements are an underestimation possibly due to concentration measurement uncertainties, slipstream flow stability, particulates, or additional C and N sources unaccounted for by our measurements, particularly with respect to C species, are discussed in the next section. On the other hand, the mass balance emissions may be overestimated because organic bio-oil that deposits within the pyrolysis system is unaccounted for as emissions. This source of error in the mass balance is lower in experiment 2 likely because of the large amount of manure run, which makes the percentage amount of bio-oil deposited on surfaces within the pyrolysis system lower. Although each approach had sources of error associated with them, the combination of the two approaches provides a range of likely emissions from chicken manure pyrolysis at these conditions.

Mass Balance and Effluent Gas Flux Uncertainties. Regression slope uncertainties are less than 0.2% during both experiments for all species with the exception of that for NO with 13% median uncertainty for experiment 1 (SI Table S4). Since regression slope uncertainties (<0.2%) were generally much lower than concentration uncertainties (≥1%), linear regression slope fitting does not introduce significant uncertainties above the concentration uncertainty levels for the majority of our gas measurements (SI Table S5). Therefore, we estimate gas flux uncertainties using the concentration uncertainties in SI Table S5 and average flux values across the experimental period. The error propagation for total N and C gas emissions results in 2.3×10^{-03} and 1.6×10^{-03} kg N and 6.8×10^{-04} and 1.5×10^{-03} kg C (for experiments 1 and 2, respectively) uncertainties that cannot account for the 50−450 g discrepancies in mass lost derived from the MB and GF methods (Figure 2). Although the 6−16 g mass balance approach uncertainties (Table 2 and SI Tables S2, S6) dominate the error bars in Figure 2, these errors also cannot account for the mass discrepancies.

We assess the potential for biases due to instability of flow rates and unmeasured C and N gases/particles to account for these discrepancies, especially for C species. The mean slipstream varied by 20% (1σ) during experiment two (SI Table S3) and could cause underestimation of gas emissions.

DOI: 10.1021/acssuschemeng.7b00815
ACS Sustainable Chem. Eng. XXXX, XXX, XXX−XXX

Altering the gas flow within this uncertainty could make up an estimated missing C mass (~0.05 kg), but not all of it (~0.36 kg would still be missing). A major source of overestimation in the mass balance approach for both C and N is bio-oil that condenses in the piping of the pyrolysis system and is therefore not recovered in the collection vessel. Additional sources of error could be C loss as noncondensable particulates we are not incorporating in our calculations or other organic C gases not measured during this study (e.g., ethylene and other light hydrocarbon gases). For N gases, NH_3 emissions are likely underestimated due to adsorption/surface reaction losses. Although the chamber walls provided a sink for NH_3, the dominant adsorption flux losses in our system were associated with the slipstream tubing/filters at ambient temperature and relative humidity before entering the flux chamber.

DISCUSSION

Production conditions and biomass feedstock are important considerations when assessing the overall potential benefits of biochar for soil quality improvements, pyrolysis coproduct yield, biomass management and environmental impact. Using fast pyrolysis, our results suggest that both experimental temperature regimes resulted in similar (~23%) biochar yields, while a slightly greater proportion of C and N gas production occurred under low temperatures (~25%) and slightly higher yields in bio-oil occurred at high temperatures (~55%) (Table 1, SI Figures S3, S4). This observation is opposite of what is normally observed under varied temperature conditions in pyrolysis studies, although the differences are very small. Other studies have found larger differences in biochar yield and nutrient properties over larger temperature ranges (300 and 600 °C), which also vary by biochar material.[14,15] The flux measurements presented here will enable progress on constraining optimal pyrolysis conditions while optimizing bio-oil and biochar yield and minimizing noxious gas emissions during manufacturing. Moreover, the release of gases implicated in climate forcing and air quality degradation are important considerations in a life cycle net cost benefit analysis and assessment of the economic feasibility of biochar production from manure.

Technologies that convert poultry manure into bioenergy and soil amendments have the potential to improve the environmental sustainability of poultry waste management from operations at small- and large-scales.[24] Poultry production is the fastest growing livestock sector globally.[25] Its intensification poses increasing challenges for best treatment and use of manure nutrients. This work has direct implications for future life cycle assessments that can compare net benefits and trade-offs of manure management practices in hotspots of concentrated chicken manure production, such as the Chesapeake Bay Watershed. Additionally, this work will provide beneficial information to aide in structuring future poultry waste management strategies, such as large-scale biochar production, which will become more important as global poultry production continues to rise. As of 2016, poultry production comprised 115.8 million tons of the 320 million tons of global meat produced annually.[26]

Of the gaseous components measured, NH_3, CO_2, and CO comprised the largest emissions during each experiment. NH_3 made up ~99% of the gaseous Nr emissions (by mass) for both experiments, while NO and N_2O contributed to less than 5% (SI Figures S2; Tables 3, 4). At the lower temperature, CO_2 comprised 66% of the total C gaseous content, while CO was 29% (Table 3). These percentages were likely observed due to reducing, anaerobic conditions or possibly hydrocarbon exchange. However, at the higher temperature CO_2 emissions dropped to 58% and CO increased to 36% of total C (Table 4). Interestingly, varying temperature conditions seemed to have an effect on the composition of CO_2 and CO present (Tables 3 and 4). Since pyrolysis is an anaerobic process, the presence of oxidized nitrogen species, such as NO, is somewhat surprising, but perhaps is a function of high moisture, mineral content or reaction with organic oxygen contained in the manure.

Manure wastes have high ammonium content, thus NH_3 volatilization was expected to occur, especially under high heat conditions and is a likely explanation for the abundance of NH_3 measured in total N yield as has been suggested in other work.[17] This result suggests that the process of producing biochar via pyrolysis could emit a substantial amount of NH_3 if manure wastes are utilized as the feedstock and gaseous emissions are not contained or reused, such as in gasification systems. High NH_3 emissions during pyrolysis may also offset potential reactive N mitigation effects of transitioning from raw manure to manure-derived biochar agricultural soil amendments.

In an effort to address the significance of these measurements, conservatively scaling up these NH_3 pyrolysis emissions to an annual production estimate, our gas flux measurements suggest that 1.4×10^{-3} to 2.7×10^{-3} kg NH_3–N would be produced from pyrolysis of one kg of manure (SI Table S9). Within the Chesapeake Bay Watershed, an estimated 8.64 billion kg of excess manure is applied in the region to agricultural soils every year.[14] According to the measurements conducted in this study, if this excess manure was turned into biochar via pyrolysis prior to land application, as much as 1.2×10^7 kg of NH_3 could be emitted into the air every year increasing the potential impact of atmospheric N deposition without a mechanism to capture the gas exhaust. However, this is potentially a better option than NH_3 volatilization from chicken manure applications onto agricultural land, which can be as high as 20–60% of the total N applied and vary with environmental conditions, such as temperature.[27] Compared with pyrolysis, emissions for chicken manure applications can be up to an order of magnitude higher ranging from 3.4×10^7 to 1.0×10^8 kg NH_3–N yr^{-1}. Within the context of the Chesapeake Bay Watershed and similar regions challenged with the management of concentrated livestock wastes, pyrolysis could minimize water pollution with reduced runoff and improve air quality. However, without a mechanism for capturing or recycling the exhaust the pyrolysis process would still emit 12–35% (SI Table S9) of what would naturally volatize from land applications of manure. Given this information, it may be more practical to implement a pollution control system on a pyrolysis plant than attempting to control emissions in agricultural fields.

While many studies have tested the utility of wood-based feedstocks for biochar production, recent attention has been focused on the benefits of biochar produced by manures, agricultural wastes, and crop biomass, which can be plentiful in the environment and challenging to dispose of properly. Biochar made from chicken manure has been found to enhance N, potassium and phosphorus availability in soils,[28,29] but may also contribute to reactive N losses to the environment when used as a soil amendment. Field experiments have also shown that crop yields increase and greenhouse gas emissions of species such as N_2O decrease when poultry char is applied to

DOI: 10.1021/acssuschemeng.7b00815
ACS Sustainable Chem. Eng. XXXX, XXX, XXX–XXX

cornfields in sandy and silty-loam agricultural plots.[6] Additionally, biochar products minimize volume and mass of the original feedstock,[12] which reduces transportation costs allowing for the transport of nutrients within and across watersheds. Enhanced capacity for transportation would alleviate N pollution hotspots.[14] Further investigations into life cycle cost-benefit analyses[15,30,31] would allow for estimating regional scale impacts of each of these factors, including production, transportation and utilization in agricultural settings, to assess its realistic applicability and role in mitigating air quality and climate impacts, nutrient leaching and promoting C sequestration.

■ ASSOCIATED CONTENT

Supporting Information

The Supporting Information is available free of charge on the ACS Publications website at DOI: 10.1021/acssuschemeng.7b00815.

Additional tables are included in the supplement and relay information discussed in the manuscript (PDF)

■ AUTHOR INFORMATION

Corresponding Author

*E-mail: ryals@hawaii.edu.

ORCID

Rebecca Ryals: 0000-0002-4394-9027
Charles A. Mullen: 0000-0001-5739-5451
Mark A. Zondlo: 0000-0003-2302-9554

Notes

The authors declare no competing financial interest.

■ ACKNOWLEDGMENTS

This work was made possible by funding provided by the Institute at Brown for Environment and Society (IBES) Seed Grant Program (to MGH and RR) and the Rathmann Family Foundation (to RR). Special thanks to all assistance and support provided by the United States Department of Agriculture Sustainable Biofuels and Co-Products Division at the Eastern Regional Research Center, Mark Schaffer, Tom Coleman, Craig Einfeldt, Frye Poultry, the Tang Lab at the Marine Biological Laboratory, Elizabeth de la Reguera, Lei Tao, Los Gatos Research, Joseph Orchardo, Dave Murray, Ruby Ho, and Paul Wotjal. We also thank three anonymous reviewers for constructive feedback on the manuscript. Mention of trade names or commercial products in this publication is solely for the purpose of providing specific information and does not imply recommendation or endorsement by the U.S. Department of Agriculture. USDA is an equal opportunity provider and employer.

■ REFERENCES

(1) IPCC. *Climate Change 2013: The Physical Science Basis. Contribution of Working Group I to the Fifth Assessment Report of Intergovernmental Panel on Climate Change*; Stocker, T. F.; Qin, D.; Plattner, G. K.; Tignor, M.; Allen, S. K.; Boschung, J.; Nauels, A.; Xia, Y.; Bex, V.; Midgley, P. M., Eds.; Cambridge University Press: Cambridg, 2013; DOI: 10.1017/CBO9781107415324.

(2) Fowler, D.; Coyle, M.; Skiba, U.; Sutton, M. A.; Cape, J. N.; Reis, S.; Sheppard, L. J.; Jenkins, A.; Grizzetti, B.; Galloway, J. N.; Vitousek, P.; Leach, A.; Bouwman, A. F.; Butterbach-Bahl, K.; Dentener, F.; Stevenson, D.; Amann, M.; Voss, M. The global nitrogen cycle in the twenty-first century. *Philos. Trans. R. Soc., B* **2013**, *368*, 20130164.

(3) Nguyen, B.; Koide, R. T.; Dell, C.; Drohan, P.; Skinner, H.; Adler, P. R.; Nord, A. Turn-over of soil carbon following addition of switchgrass-derived biochar to four soils. *Soil Sci. Soc. Am. J.* **2014**, *78*, 531.

(4) Hansen, V.; Muller-Stover, D.; Ahrenfeldt, J.; Holm, J. K.; Henriksen, U. B.; Hauggaard Nielsen, H. Gasification biochar as a valuable by-product for carbon sequestration and soil amendment. *Biomass Bioenergy* **2015**, *72*, 300−308.

(5) Crombie, K.; Masek, O. Pyrolysis biochar systems, balance between bioenergy and carbon sequestration. *GCB Bioenergy* **2015**, *7*, 349−361.

(6) Ryals, R. A.; Tang, J.; Hastings, M. G.; King, D.; Castner, E.; Teller, A.; Clark, M.; Porder, S.; Almaraz, M.; Dell, C.; Sim, T. Can biochar reduce nitrogen pollution from manure? Assessing biochar's biogeochemical fate and policy opportunities. *Ecol. Soc. Am.* **2015** Conference Talk.

(7) Zhang, Y.; Lin, F.; Wang, X.; Zou, J.; Liu, S. Annual accounting of net greenhouse gas balance response to biochar addition in a coastal saline bioenergy cropping system in China. *Soil Tillage Res.* **2016**, *158*, 39−48.

(8) Pandey, V.; Patel, A.; Patra, D. D. Biochar ameliorates crop productivity, soil fertility, essential oil yield and aroma profiling in basin (Ocimum basilicum L.). *Ecol. Eng.* **2016**, *90*, 361−366.

(9) Koide, R. T.; Nguyen, B. T.; Skinner, R. H.; Dell, C. J.; Peoples, M. S.; Adler, P. R.; Drohan, P. J. Biochar amendment of soil improves resilience to climate change. *GCB Bioenergy* **2015**, *7*, 1048−1091.

(10) Taghizadeh-Toosi, A.; Clough, T. J.; Sherlock, R. R.; Condron, L. M. Biochar adsorbed ammonia is bioavailable. *Plant Soil* **2012**, *350*, 57−69.

(11) Troy, S. M.; Lawlor, P. G.; O'Flynn, C. J.; Healy, M. G. The impact of biochar addition on nutrient leaching and soil properties from tillage soil amended with pig manure. *Water, Air, Soil Pollut.* **2014**, *225*, 1900.

(12) Lima, I. M.; Boateng, A. A.; Klasson, T. K. Pyrolysis of broiler manure: char and product gas characterization. *Ind. Eng. Chem. Res.* **2009**, *48*, 1292−1297.

(13) Boateng, A. A.; Daugaard, D. E.; Goldberg, N. M.; Hicks, K. B. Bench-scale fluidized bed pyrolysis of switchgrass for bio-oil production. *Ind. Eng. Chem. Res.* **2007**, *46*, 1891−1897.

(14) Kleinman, P.; Saack Blunk, K.; Bryant, R.; Saporito, L.; Beegle, D.; Czymmek, K.; Ketterings, Q.; Sims, T.; Shortle, J.; McGrath, J.; Coale, F.; Dubin, M.; Dostie, D.; Maguire, R.; Meinen, R.; Allen, A.; O'Neill, K.; Garber, L.; Davis, M.; Clark, B.; Sellner, K.; Smith, M. Managing manure for sustainable livestock production in the Chesapeake Bay Watershed. *J. Soil Water Conserv.* **2012**, *67* (2), 54A−61A.

(15) Pourhashem, G.; Spatari, S.; Boateng, A. A.; McAloon, A. J.; Mullen, C. A. Life cycle environmental and economic tradeoffs of using fast pyrolysis products for power generation. *Energy Fuels* **2013**, *27*, 2578−2587.

(16) Galloway, J. N.; Aber, J. D.; Willem Erisman, J.; Seitzinger, S. P.; Howarth, R. W.; Cowling, E. B.; Cosby, J. B. *BioScience* **2003**, *53* (4), 341−356.

(17) Zhou, J.; Masutani, M.; Ishimura, D. M.; Turn, S. Q.; Kinoshita, C. M. Release of fuel-bound nitrogen during biomass gasification. *Ind. Eng. Chem. Res.* **2000**, *39* (3), 626−634.

(18) Frye, J. 2017. *Personal communication.*

(19) Huber, G. W.; Iborra, S.; Corma, A. Synthesis of transportation fuels from biomass: chemistry, catalysts, and engineering. *Chem. Rev.* **2006**, *106*, 4044−4098.

(20) Coti, R.; Fabbri, D.; Vassura, I.; Ferroni, L. Comparison of chemical and physical indices of thermal stability of biochars from different biomass by analytical pyrolysis and thermogravimetry. *J. Anal. Appl. Pyrolysis* **2016**, *122*, 160−168.

(21) Miller, D. J.; Sun, K.; Tao, L.; Khan, M. A.; Zondlo, M. A. Open-path, quantum cascade-laser-based sensor for high resolution atmospheric ammonia measurements. *Atmos. Meas. Tech.* **2014**, *7*, 81−93.

DOI: 10.1021/acssuschemeng.7b00815
ACS Sustainable Chem. Eng. XXXX, XXX, XXX−XXX

(22) Laville, P.; Lehuger, S.; Loubet, B.; Chaumartin, F.; Cellier, P. Effect of management, climate and soil conditions on N2O and NO emissions from an arable crop rotation using high temporal resolution measurements. *Agric. & For. Meteorol.* **2011**, *151*, 228−240.
(23) MATLAB 8.6, The MathWorks Inc., Natick, MA, R2015b.
(24) Williams, C. M. Poultry waste management in developing countries. FAO: *Poultry Development Review*. 2013. http://www.fao.org/docrep/019/i3531e/i3531e05.pdf.
(25) FAO. Forward. *Poultry Development Review*. 2013. http://www.fao.org/docrep/019/i3531e/i3531e01.pdf.
(26) FAO. Food outlook: biannual report on global food markets. October 2016. http://www.fao.org/3/a-i6198e.pdf.
(27) Pote, D. H.; Meisinger, J. J. Effect of poultry litter application method on ammonia volatilization from a conservation tillage system. *J. Soil Water Conserv.* **2014**, *69*, 1.
(28) Chan, K. Y.; Van Zwieten, L.; Meszaros, I.; Downie, A.; Joseph, S. Using poultry litter biochars as soil amendments. *Aust. J. Soil Res.* **2008**, *46*, 437−444.
(29) Ro, K. S.; Cantrell, K. B.; Hunt, P. G. High-temperature pyrolysis of blended animal manures for producing renewable energy and value-added biochar. *Ind. Eng. Chem. Res.* **2010**, *49*, 10125−10131.
(30) Delonge, M. S.; Ryals, R. A.; Silver, W. L. A lifecycle model to evaluate carbon sequestration potential and greenhouse gas dynamics of managed grasslands. *Ecosystems* **2013**, *16*, 962−979.
(31) Wu, H.; Hanna, M. A.; Jones, D. D. Life cycle assessment of greenhouse gas emissions of feedlot manure management practices: Land application versus gasification. *Biomass Bioenergy* **2013**, *54*, 260−266.

DOI: 10.1021/acssuschemeng.7b00815
ACS Sustainable Chem. Eng. XXXX, XXX, XXX−XXX